

RESEARCH ARTICLE

# An aerosol challenge model of tuberculosis in Mauritian cynomolgus macaques

S. A. Sharpe<sup>1\*</sup>, A. D. White<sup>1</sup>, L. Sibley<sup>1</sup>, F. Gleeson<sup>2</sup>, G. A. Hall<sup>1</sup>, R. J. Basaraba<sup>3</sup>, A. McIntyre<sup>2</sup>, S. O. Clark<sup>1</sup>, K. Gooch<sup>1</sup>, P. D. Marsh<sup>1</sup>, A. Williams<sup>1</sup>, M. J. Dennis<sup>1</sup>

**1** Public Health England, National Infection Service, Porton Down, Salisbury, SP4 0JG, United Kingdom, **2** The Churchill Hospital, Headington, Oxford, United Kingdom, **3** Department of Microbiology Immunology and Pathology, College of Veterinary Medicine and Biomedical Sciences, Colorado State University, Fort Collins, Colorado, United States of America

\* [sally.sharpe@phe.gov.uk](mailto:sally.sharpe@phe.gov.uk)

## Abstract

### Background

New interventions for tuberculosis are urgently needed. Non-human primate (NHP) models provide the most relevant pre-clinical models of human disease and play a critical role in vaccine development. Models utilising Asian cynomolgus macaque populations are well established but the restricted genetic diversity of the Mauritian cynomolgus macaques may be of added value.

### Methods

Mauritian cynomolgus macaques were exposed to a range of doses of *M. tuberculosis* delivered by aerosol, and the outcome was assessed using clinical, imaging and pathology-based measures.

### Results

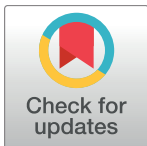
All macaques developed characteristic clinical signs and disease features of tuberculosis (TB). Disease burden and the ability to control disease were dependent on exposure dose. Mauritian cynomolgus macaques showed less variation in pulmonary disease burden and total gross pathology scores within exposure dose groups than either Indian rhesus macaques or Chinese cynomolgus macaques

### Conclusions

The genetic homogeneity of Mauritian cynomolgus macaques makes them a potentially useful model of human tuberculosis.

## 1. Introduction

*Mycobacterium tuberculosis* (*M. tuberculosis*), the causative agent of tuberculosis (TB), is responsible for 9 million new infections and 1.5 million deaths each year [1]. Tuberculosis is



## OPEN ACCESS

**Citation:** Sharpe SA, White AD, Sibley L, Gleeson F, Hall GA, Basaraba RJ, et al. (2017) An aerosol challenge model of tuberculosis in Mauritian cynomolgus macaques. PLoS ONE 12(3): e0171906. doi:10.1371/journal.pone.0171906

**Editor:** Zandrea Ambrose, University of Pittsburgh, UNITED STATES

**Received:** October 4, 2016

**Accepted:** January 27, 2017

**Published:** March 8, 2017

**Copyright:** © 2017 Sharpe et al. This is an open access article distributed under the terms of the [Creative Commons Attribution License](https://creativecommons.org/licenses/by/4.0/), which permits unrestricted use, distribution, and reproduction in any medium, provided the original author and source are credited.

**Data Availability Statement:** All relevant data are within the paper.

**Funding:** This work was supported by the Department of Health, UK.

**Competing interests:** The authors have declared that no competing interests exist.

an enormous global health issue due to the rise in drug-resistant strains, the impact of co-infection with HIV, and the estimate that a third of the world's population could be latently infected. Vaccination is widely accepted to be the most effective method for infectious disease control, and although the only licenced vaccine against *M. tuberculosis*, Bacille Calmette-Gur in (BCG), protects children from developing severe TB disease [2], the protection afforded to adults is limited [3], and it is unsuitable for use in people whose immune system is compromised, so more effective vaccines against *M. tuberculosis* are desperately needed.

Preclinical animal models are critical to the development of new vaccines, as studies of infectious challenge can be used to predict the effectiveness of vaccines in humans and they provide the opportunity to identify and validate correlates of protection. Due to their close similarity to humans, non-human primates offer the most relevant models of human diseases, and models of *M. tuberculosis* have been established in both rhesus macaque (*Macaca mulatta*) and cynomolgus macaque (*Macaca fascicularis*) species [4–6] with cynomolgus macaques showing an improved ability to control *M. tuberculosis*-induced disease [7, 8]. To date, the cynomolgus macaque models reported have employed Asian cynomolgus macaques from either China or the Philippines [9–12] and studies have shown these populations to exhibit a full spectrum of outcomes to *M. tuberculosis* challenge, from latent infection to the development of active progressive disease [4], which is likely to be a reflection of their wide genetic diversity.

Cynomolgus macaques are indigenous to mainland Southeast Asia, and surrounding islands such as Sumatra and the Philippines, but have also been introduced as an alien species in several locations, including the island of Mauritius. The Mauritian cynomolgus macaque population that descended from the small founder group consequently show a reduced genetic variability [13]. Consequently, differences in genetic composition [14] and phenotypic characteristics, such as body weight [15], sexual maturation rate [16], blood chemistry and haematology [17], and microbiome [18] compared with populations from within the species natural range of habitats in Asia have been reported. Furthermore, developments in the immunogenetic characterisation of Mauritian cynomolgus macaques have identified their value in the study of the role of host MHC genetics in immunogenicity and vaccine studies [19–27]. Thus, the Mauritian cynomolgus macaque has the potential to provide an important addition to the portfolio of macaque models of *M. tuberculosis*. A less genetically diverse population may, respond more reproducibly to infection, enhancing the ability to discriminate protective effects afforded by new vaccine candidates and facilitate the identification of much needed immune correlates of protection. The pilot study reported here aimed to establish an aerosol challenge model of TB in Mauritian cynomolgus macaques, and evaluate the effect of different challenge doses of *M. tuberculosis* on the clinical outcome.

## 2. Materials and methods

### 2.1 Experimental animals

Nine captive-bred cynomolgus macaques of Mauritian genotype aged between 2 and 4 years were obtained from an established UK breeding colony [28]. Absence of previous exposure to mycobacterial antigens (*M. tuberculosis* infection or environmental mycobacteria) was confirmed by the tuberculin test whilst the animals were still in their original breeding colony, and just prior to study start, by the IFN- $\gamma$  based Primagam<sup>™</sup> test kit (Biocor Animal Health Inc, Omaha, Nebraska, USA) and an *ex-vivo* IFN- $\gamma$  ELISPOT (Mabtech AB, Nacka Strand, Sweden) to measure responses to mycobacterial antigens: PPD (Statens Serum Institute, Copenhagen, Denmark), and pooled 15-mer peptides of ESAT6 and CFP10 (Peptide Protein Research LTD, Fareham, UK). Animals were housed in compatible social groups, in accordance with

the Home Office (UK) Code of Practice for the Housing and Care of Animals Used in Scientific Procedures (1989), and the National Committee for Refinement, Reduction and Replacement (NC3Rs) Guidelines on Primate Accommodation, Care and Use, August 2006 (NC3Rs, 2006) in cages approximately 2.5M high by 4M long by 2M deep. These cages were constructed with high level observation balconies and with a floor of deep litter to allow foraging. Further enrichment was afforded by the provision of toys, swings, feeding puzzles and DVDs for visual stimulation. In addition to standard old world primate pellets further food was provided by a selection of vegetables and fruit. Animals were sedated by intramuscular injection of ketamine hydrochloride (Ketaset, 100mg/ml, Fort Dodge Animal Health Ltd, Southampton, UK; 10mg/kg) for procedures requiring their removal from their housing. None of the animals had been used previously for experimental procedures and each socially compatible group was randomly assigned to a particular study treatment. All animal procedures and study design were approved by the Public Health England, Porton Down Ethical Review Committee, and authorized under an appropriate UK Home Office project license.

## 2.2 *M. tuberculosis* strain

The *M. tuberculosis* Erdman strain K01 used for challenge was provided by the CBER/FDA repository and prepared from frozen suspensions at a stated titre of  $3.5 \pm 1.5 \times 10^8$  CFU/ml. For challenge, sufficient vials were thawed and diluted appropriately, as stated below, in sterile distilled water.

## 2.3 Aerosol exposure

Macaques were challenged by exposure to aerosols of *M. tuberculosis* as previously described [29–31]. Mono-dispersed bacteria in particles were generated using a 3-jet Collison nebuliser (BGI) and, in conjunction with a modified Henderson apparatus [32], delivered to the nares of each sedated primate via a modified veterinary anaesthetic mask. Challenge was performed on sedated animals placed within a ‘head-out’, plethysmography chamber (Buxco, Wilmington, North Carolina, USA) to enable the aerosol to be delivered simultaneously with the measurement of respired volume. The aerosol delivery process was designed to result in the deposition of a defined spread of target doses ranging from 22–250 CFU retained in the lungs (Table 1). This range of low and very high challenge doses was selected because the susceptibility of this species of macaque to TB was unknown. The number of bacilli deposited and retained in the lungs of macaques cannot be measured directly, and so quantification of the dose is calculated from the concentration of viable organisms in the aerosol ( $C_{\text{aero}}$ ) and the volume of aerosol inhaled by the animal. This ‘presented dose’ (PD) is the number of organisms that the animals inhale.  $C_{\text{aero}}$  is either measured directly using air sampling within the system or may be calculated using the concentration of organisms in the nebulizer ( $C_{\text{neb}}$ ) and a ‘spray factor’ that is a constant derived from data generated for the specific organism with identical aerosol exposure parameters. The calculations to derive the PD and the retained dose (the number of organisms assumed to be retained in the lung) have been described previously for high/medium aerosol doses [30, 31]. The assumed retained dose was calculated from the PD by applying a retention factor. Retention factors for rhesus macaques are described by Harper and Moreton [33].

## 2.4 Clinical assessment

Animals were monitored daily for behavioural abnormalities including depression, withdrawal from the group, aggression, and changes in feeding patterns, respiration rate and the occurrence of cough. Animals were weighed, rectal temperature measured and examined for gross abnormalities on each occasion that required blood sample collection, aerosol challenge or euthanasia.

**Table 1. Aerosol challenge doses of *M. tuberculosis* delivered to Mauritian cynomolgus macaques.**

Animal Identification number	Presented Dose range (CFU)	Presented Dose (CFU)	Estimated Retained Dose [30,31]. (CFU)
M982B	Very high [ $>1400$ ]	1650	236
I131B		1624	232
M651		1544	221
M284D	High [500–1400]	522	75
I319DB	Medium [250–500]	448	64
I347G		335	48
M054E		302	43
M064D		242	35
M988E	Low [ $<250$ ]	153	22

doi:10.1371/journal.pone.0171906.t001

Red blood cell (RBC) haemoglobin levels were measured using a HaemaCue haemoglobin-ometer (Haemacue Ltd, Dronfield, UK) to identify the presence of anaemia, and erythrocyte sedimentation rates (ESR) were measured using the Sediplast system (Guest Medical, Edenbridge, UK) to detect and monitor inflammation induced by infection with *M. tuberculosis*.

The time of necropsy, if prior to the end of the planned study period, was determined by experienced primatology staff and based on a combination of the following adverse indicators: depression or withdrawn behaviour, abnormal respiration (dyspnoea), loss of 20% of peak post-challenge weight, ESR levels elevated above normal ( $>20$  mm), haemoglobin level below normal limits ( $<100$ g/dL), increased temperature ( $>41$  °C) and abnormal thoracic radiograph. The range of adverse indicators used allowed application of humane intervention when individuals had progressed to moderate disease.

## 2.5 Immune response analysis

**2.5.1 Interferon-gamma (IFN- $\gamma$ ) ELISpot.** The *M. tuberculosis*-specific immune response was evaluated at two weekly intervals throughout the study. Peripheral blood mononuclear cells were isolated from heparin anti-coagulated blood using standard methods. An IFN- $\gamma$  ELISpot assay was used to estimate the numbers and IFN- $\gamma$  production capacity of mycobacteria-specific T cells in PBMCs using a human/simian IFN- $\gamma$  kit (Mabtech AB, Nacka Strand, Sweden), as described previously [30]. Cells were stimulated with PPD (10  $\mu$ g/ml, SSI, Copenhagen, Denmark) or pools of overlapping 15mer peptides spanning CFP10, or ESAT6 (Peptide Protein Research Ltd, Wickham, UK).

**2.5.2 Quantification of secreted IFN- $\gamma$ .** IFN- $\gamma$  production was measured using a whole blood ELISA as previously described [30]. In brief, heparinised blood was diluted 1 in 10 with serum-free medium (RPMI supplemented with L-glutamine, penicillin and streptomycin) and cultured with purified protein derivative from *M. tuberculosis* (PPD; 5  $\mu$ g/ml, SSI, Copenhagen, Denmark), or mitogen Phytohaemagglutinin (PHA; Sigma-Aldrich, Dorset, UK) (5 $\mu$ g/l), or in medium alone for 6 days. Supernatants were harvested at day 6 and stored at -80 °C. The quantity of IFN- $\gamma$  in the supernatants was estimated using a commercially available human/monkey IFN- $\gamma$  ELISA kit (Mabtech AB, Nacka Strand, Sweden). A purified human IFN- $\gamma$  was used for the standard curve on each plate. The ELISA was developed using streptavidin and 3,3',5,5'-tetramethylbenzidine (TMB) liquid substrate system (Sigma-Aldrich, Dorset, UK) and the reaction stopped with 2M sulphuric acid (May & Baker Ltd, Dagenham, UK). ELISA plates were read at 450nm. A standard curve was plotted for each plate and used to calculate the concentrations of IFN- $\gamma$  in each sample.

## 2.6 Necropsy

Prior to euthanasia by intra-cardiac injection of a lethal dose of anaesthetic (Dolethal, Vétquinol UK Ltd, 140mg/kg), animals were anaesthetised and clinical data collected. Blood samples were taken. A post-mortem examination was performed immediately and gross pathological changes were scored using an established system based on the number and extent of lesions present in the lungs, spleen, liver, kidney and lymph nodes, as described previously [30, 31]. Samples of spleen, liver, kidneys and tracheobronchial, inguinal and axillary lymph nodes were removed and sampled for quantitative bacteriology. The lungs, including the heart and lung-associated lymph nodes, were removed intact and the lymph nodes examined for lesions. The complete lung set was fixed by intra-tracheal infusion with 10% neutral buffered formalin (NBF) using a syringe and 13CH Nelaton catheter (J.A.K. Marketing, York, UK). The catheter tip was inserted into each bronchus in turn via the trachea; the lungs were infused until they were expanded to a size considered to be normal inspiratory dimensions, and the trachea ligated to retain the fluid. The infused lung was immersed in 10% NBF. In addition, samples of kidneys, liver, spleen, and sub-clavicular, hepatic inguinal and axillary lymph nodes were fixed in 10% NBF.

## 2.7 Lung imaging

Thoracic radiographs (SP VET 3.2, Xograph Ltd) were acquired using mammography film (Xograph Imaging Systems Ltd, Tetbury, UK) before and every 2 weeks after exposure to *M. tuberculosis*. Evaluation of disease was performed by an experienced consultant thoracic radiologist blinded to the exposure dose and clinical status using a pre-determined scoring system based on the amount and distribution of infiltrate as previously described [31].

## 2.8 Magnetic resonance (MR) imaging

The *ex-vivo* expanded, fixed lungs were set in 2% agarose (Sigma-Aldrich, UK) and images were collected using a 3.0 T 750 MR Scanner (General Electric Healthcare, Milwaukee, WI, USA) as described previously [31]. This enabled evaluation of the pulmonary disease burden at the end of the study period. Lung lesions were identified in MR images from their signal intensity and nodular morphology relative to normal lung parenchyma.

## 2.9 Lesion analysis / quantification (stereology)

Lung lesions were identified on MR images based on their signal intensity and nodular morphology relative to more normal lung parenchyma. The total lung and lesion volume relative to the fixed tissue was determined using the Cavalieri method applied to MRI image stacks, and then expressed as a ratio to provide a measure of disease burden in each animal, as previously described [30, 31]. Analyses of lesion volume on MR images were performed with the investigators reading the images blind to treatment groups.

## 2.10 Pathology studies

**2.10.1 Gross examination following fixation.** The fixed lungs were sliced serially and lesions counted as described previously<sup>31</sup>. Each lung lobe was evaluated separately and discrete lesions in the parenchyma were counted. Where lesions had coalesced, these were measured and recorded. Lung-associated lymph nodes, particularly around the tracheal bifurcation, were dissected and examined. The remaining tissues were examined during trimming.

**2.10.2 Histopathological examination.** Representative samples from each lung lobe and other organs were processed to paraffin wax, sectioned at 3–5  $\mu\text{m}$ , and stained with haematoxylin and eosin (HE). For each lung lobe, tissue slices containing obvious lesions were chosen

for histological examination. Where gross lesions were not visible, a sample was taken from a pre-defined anatomical location from each lobe to establish consistency between animals. The nature and severity of the microscopic lesions was evaluated subjectively by a pathologist who was blinded to the treatment groups to prevent bias. Lesions were classified according to the scheme used by Lin [34]. In non-pulmonary tissue, the occurrence of tuberculosis induced lesions was scored as present or absent.

## 2.11 Bacteriology

The spleen, kidneys, liver and tracheobronchial lymph nodes were sampled for the presence of viable *M. tuberculosis* post-mortem<sup>31</sup>. Where available, tissue sections with and without visible tuberculous lesions were collected for analysis. Weighed tissue samples were homogenized in 2 ml of sterile water, and either serially diluted in sterile water prior to being plated or plated undiluted directly onto Middlebrook 7H11 OADC selective agar. Plates were incubated for three weeks at 37°C and resultant colonies were confirmed as *M. tuberculosis* and counted. Mean Colony forming unit (CFU) per gram from each tissue sample were determined.

## 2.12 Statistical analyses

Differences in the pathology scores, pulmonary disease measures and clinical measures of disease burden at the end of study were compared between test groups using the non-parametric Mann-Whitney U test, in Graphpad Prism, version 5.01 (GraphPad Software Inc, La Jolla, California, USA). The Spearman correlation test was used to determine the level of correlation between study parameters using GraphPad Prism, version 5.01 (GraphPad Software Inc, La Jolla, California, USA).

## 3. Results

### 3.1 *M. tuberculosis* exposure and disease progression post-challenge

Nine Mauritian cynomolgus macaques were exposed to aerosols containing a planned wide spread of estimated retained doses of *M. tuberculosis* ranging from 22–236 CFU (Table 1) and monitored for changes in behaviour and clinical parameters for up to 13 weeks after challenge. Disease progressed in five of nine animals to a level that met the humane endpoint criteria for moderate disease. In the three macaques (M982B, I131B, M651) that received the very high estimated retained aerosol doses of *M. tuberculosis* (236, 232, and 221 CFU), disease progressed rapidly and they were euthanized six or seven weeks after challenge. In the days prior to euthanasia, all three animals showed changes in their behaviour, including reduction in feeding and drinking, increased respiratory rates, ruffled coat condition. Two of the three (M982B and I131B) also became withdrawn or depressed and coughing was observed (Table 2). All three macaques also showed abnormal thoracic radiographs and clinical parameters that deviated from normal ranges that included weight loss, anaemia, and increased ESR (Fig 1).

The macaques which received the six lower doses of *M. tuberculosis* developed increased respiratory rates between week 6 and 12 after aerosol exposure and cough during weeks seven, eight and nine. Ten weeks after challenge, macaque M284D, who received a high estimated retained dose (75 CFU) of *M. tuberculosis*, was euthanized as the level of disease had progressed to meet humane end point criteria. The five macaques that were exposed to medium or low doses of *M. tuberculosis* exhibited normal behaviour and changes in weight, haemoglobin level, temperature ESR that did not exceed the normal limits, although abnormalities were detected on thoracic radiographs (Fig 1). These five animals were euthanized as planned, during the 12<sup>th</sup> (M988E, I319D, I347G) or 13<sup>th</sup> (M054E, M064D) week after challenge. Macaque

**Table 2. Contra-indicators observed in cynomolgus macaques of Mauritian origin following aerosol infection with *M. tuberculosis*.**

Animal I. D.	Estimated Retained Dose <i>M. tuberculosis</i>	Indicators observed post challenge. (week post challenge indicator recorded)		Indicators observed prior to euthanasia			
		Respiration rate	Cough	Behaviour	Eating / drinking	Respiration rate Under sedation	Other indicators
M982B	236	Rapid (5–6)	Yes (8)	Depressed withdrawn	No / No	Rapid / Shallow	Very ruffled coat. Thin
I131B	232	Rapid (5–6)	Yes (5)	Depressed	No / No	Rapid / Shallow	Very ruffled coat
M651	221	Rapid (5–6)	No	Normal	No / No	Rapid / Laboured	Ruffled coat, Thin
M284D	75	Rapid (6–10)	Yes (6, 7, 8)	Normal	Normal	Rapid / Shallow	NAD
I319DB	64	Rapid (7–12)	Yes (6, 7, 8)	Normal	Normal	Rapid laboured	NAD
I347G	48	Rapid (6–12)	Yes (6, 7, 8)	Normal	Normal	Rapid / Shallow	NAD
M054E	43	Rapid (7–12)	Yes (6, 7, 8)	Normal	Normal	Normal	NAD
M064D	35	Rapid (7–12)	Yes (6, 7, 8)	Normal	Normal	Normal	NAD
M988E	22	Rapid (7–12)	Yes (6, 7, 8)	Depressed Withdrawn	Normal	Rapid	NAD

NAD: No abnormalities detected.

doi:10.1371/journal.pone.0171906.t002

M988E, that was exposed to the lowest dose of *M. tuberculosis* (22 CFU), became withdrawn and on the day of euthanasia, exhibited chronic anaemia and a body weight loss in line with endpoint criteria.

### 3.2 IFN- $\gamma$ response following aerosol challenge with *M. tuberculosis*

The *Mycobacterium*-specific IFN- $\gamma$  response was measured by ELISpot (Fig 2A, 2B and 2C) and ELISA (Fig 2D) applied at two weekly intervals throughout the study. High frequencies of IFN- $\gamma$  producing cells measured by ELISpot were detected four to six weeks after challenge in the three macaques (M982B, I131B, M651) exposed to the highest doses of *M. tuberculosis*. The peak response to PPD was detected six weeks after challenge, while the highest responses to ESAT6 and CFP10 were measured four weeks after challenge; however, responses to these two antigens were not measured at week six in these three animals as cells were not available. Of the six macaques exposed to the lower doses, responses remained low until ten or twelve weeks after challenge, when M988E and M064D made responses above pre-infection levels to all three antigens, in contrast I319DB responded to ESAT6 and CFP10 but not PPD, while M284D responded to CFP10 and PPD. Responses to PPD, ESAT6 or CFP10 above pre-infection levels were not detected in I347G and M054E following exposure to *M. tuberculosis*.

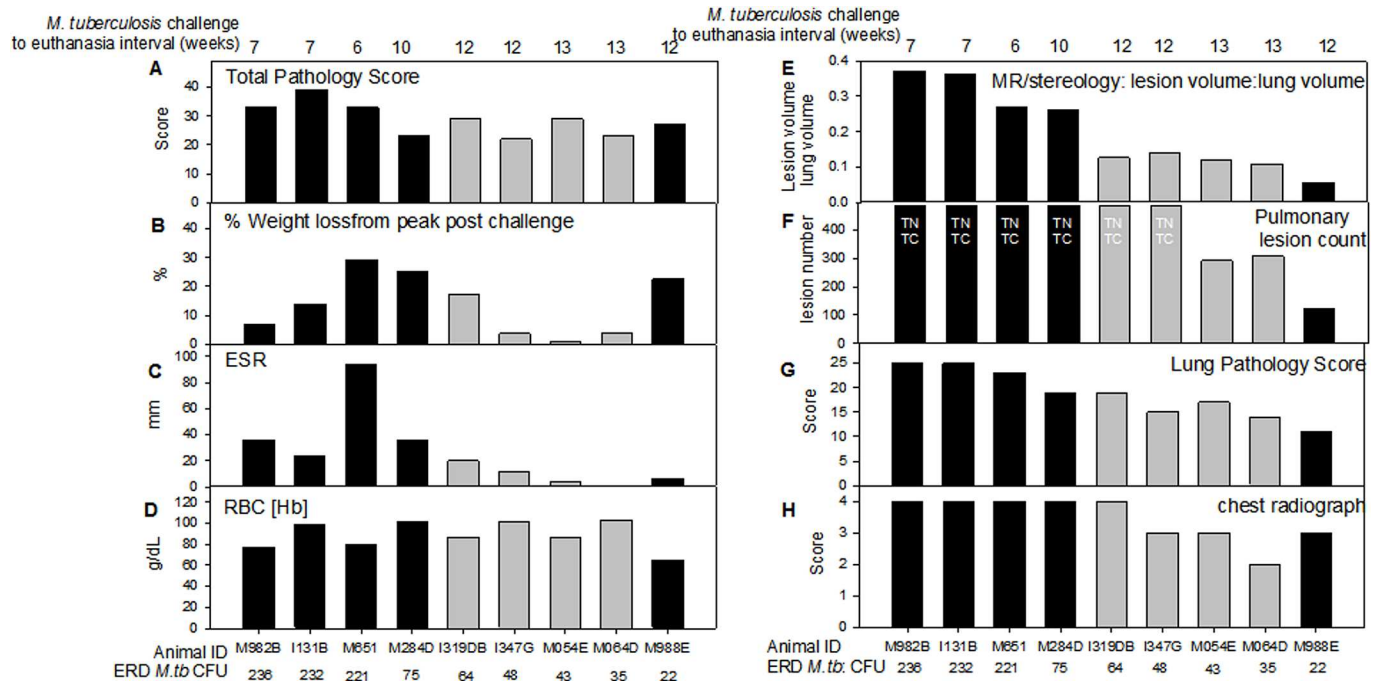


**Fig 1. Measures of pulmonary disease and clinical disease severity in Mauritian cynomolgus macaques following aerosol exposure to a range of doses of *M. tuberculosis*.** Black fill colour represents animals in which disease progressed rapidly and met endpoint criteria prior to the end of the study. Panel A: the total pathology score determined using a quantitative scoring system; Panel B: % weight loss from peak post-challenge weight on the day of euthanasia; Panel C: Erythrocyte sedimentation rate (ESR) on the day of euthanasia, or seven days prior to euthanasia (M982B, I131B, M988E); Panel D: Red blood cell haemoglobin concentration (RBC[Hb]) on the day of euthanasia; Panel E: the lung to lesion volume ratio determined using MR stereology; Panel F: number of lesions in the lung enumerated by serial sectioning and manual counting; Panel G: the scores attributed to the pulmonary component as part of the total pathology score; Panel H: score attributed to the chest radiograph on the day of euthanasia; TNTC indicates too numerous to count.

doi:10.1371/journal.pone.0171906.g001

Evaluation by ELISA of blood collected from M064D at four, six and ten weeks and from M284D at four weeks after challenge, produced high levels of IFN- $\gamma$  following stimulation with PPD, which was in contrast to the very low levels secreted by blood collected from the other seven animals during the study.

### 3.3 Measures of tuberculosis-induced disease burden

At the end of the study, the level of *M. tuberculosis*-induced disease burden was determined using a range of approaches that have been used previously for the evaluation of TB disease in both rhesus [30, 31] and cynomolgus macaques [31] (Fig 1). *M. tuberculosis*-induced disease burden measured by total pathology score (Fig 1A) and the clinical markers of weight loss (Fig 1B), increased in ESR (Fig 1C) and reduction in red blood cell haemoglobin concentration (Fig 1D) showed non-significant trends to be higher in the four animals exposed to very high, or high aerosol doses of *M. tuberculosis* relative to those receiving lower dose challenge. Furthermore, these high and very high dose animals developed symptoms indicative of progressive disease and met humane endpoint criteria, whilst the five animals exposed to lower doses controlled disease progression to the end of the study.

The level of pulmonary disease measured by MR stereology, gross pathology score and chest radiograph score was significantly higher in the four macaques that were exposed to very high or high challenge doses than in the macaques exposed to medium or low doses of *M. tuberculosis* (MR stereology:  $p = 0.0159$ , gross pathology score:  $p = 0.0238$ , chest radiograph



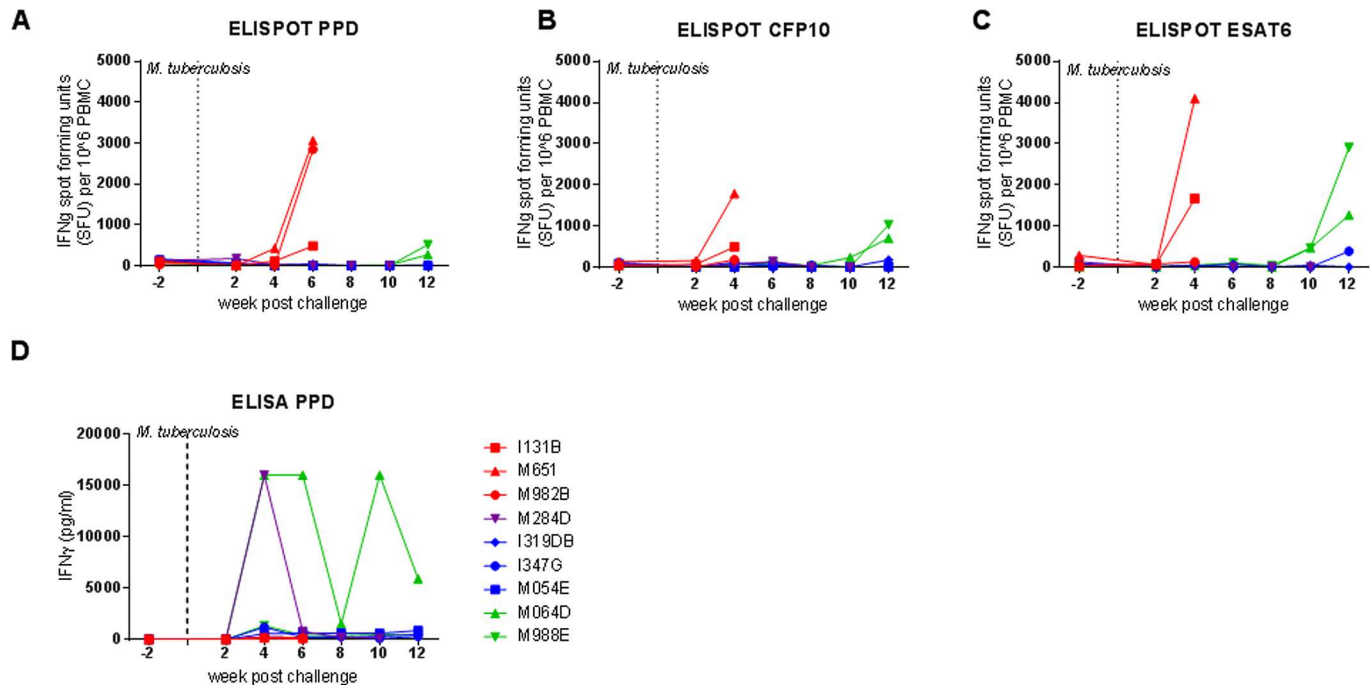


**Fig 2. Immune responses after aerosol challenge with *M. tuberculosis*.** The frequency of *Mycobacterium*-specific IFN- $\gamma$  secreting cells measured after challenge by ELISpot is shown in panels A (PPD), B (CFP10) and C (ESAT6). Panel D shows the profile of IFN- $\gamma$  secretion by PPD-stimulated whole blood measured by ELISA. Exposure to *M. tuberculosis* at week 0 is indicated by the dotted line.

doi:10.1371/journal.pone.0171906.g002

score:  $p = 0.0479$ ) and increased in line with the exposure dose (Fig 1E–1H). The Spearman’s Rank correlation test revealed significant relationships between exposure dose and lung disease burden quantified by MR stereology ( $p < 0.0001$ ,  $r = 0.9833$ ), lung gross pathology ( $p < 0.0001$ ,  $r = 0.9748$ ), chest radiograph score ( $p = 0.0079$ ,  $r = 0.8572$ ), ESR ( $p = 0.0028$ ,  $r = 1.00$ ) (Fig 3A, 3B, 3C and 3D) and survival time after challenge (Fig 2E). Three-dimensional images constructed from the MR scans demonstrated the relationship between disease burden and exposure dose and showed the lesions to be evenly distributed throughout all of the lobes of the lung (Fig 4). Macroscopic examination confirmed the pulmonary lesions in animals exposed to higher doses of *M. tuberculosis*, to be more severe than in animals receiving lower dose challenge (Table 3). An atypical combination of mature mild lesions with very numerous, small miliary lesions was noted in animal M988E.

Sections of lung, hilar lymph node, liver, hepatic lymph node, kidney and spleen from all nine animals were microscopically examined for the presence of tuberculous lesions, and granulomas were classified according to the scheme used by Lin *et al* [34] (Table 4). Tuberculous granulomas varying in nature from unorganised to caseated were detected in all animals; caseated lesions were more extensive in animals that received the higher doses. Calcification of caseated tissue was observed in I319DB (lung), M064D (lung) and M988E (spleen). M988E was exceptional, in that superimposed on the caseated granulomas was what appeared to be a more recent development of numerous, small, multifocal granuloma, principally present in lung, liver and kidney.

### 3.4 Extra-pulmonary organ-specific bacterial burden

The level of bacterial burden was evaluated in the liver, spleen, kidneys and hilar lymph nodes in all animals. A similar frequency of isolation from tissues and level of bacterial burden was

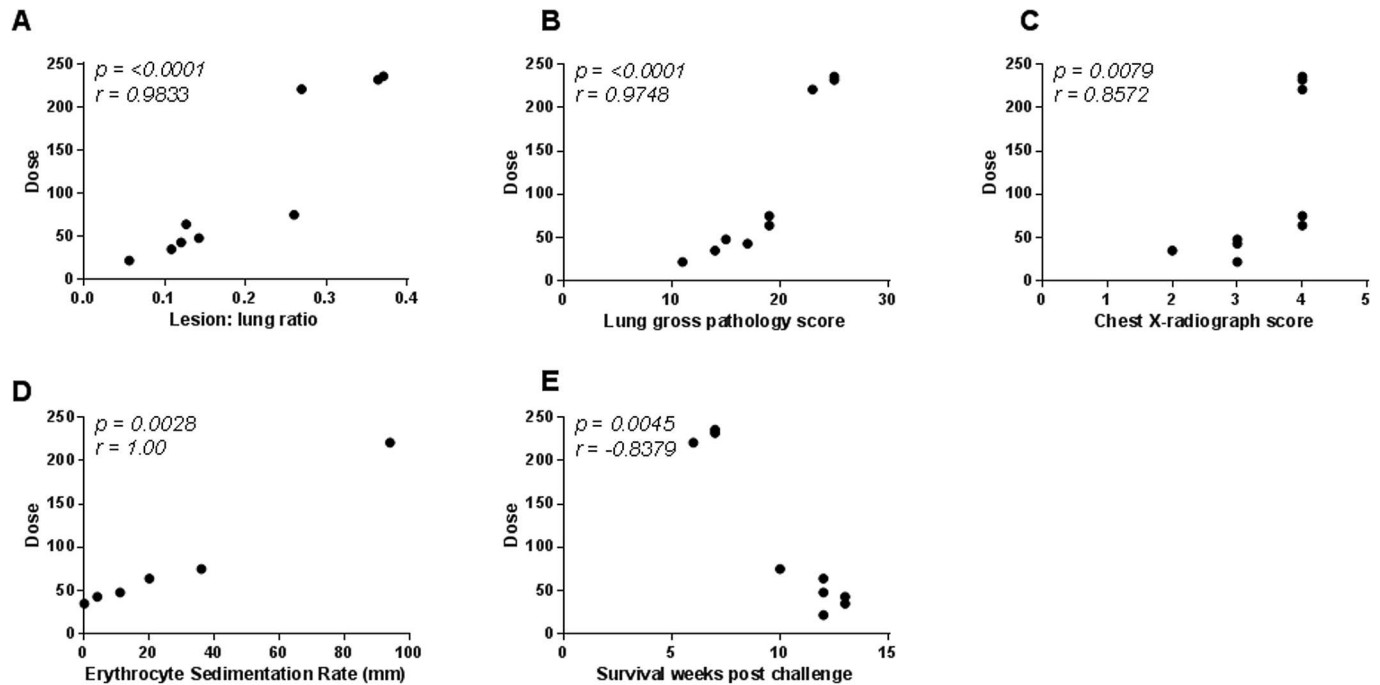


**Fig 3.** Correlation plots comparing the challenge dose (estimated retained) of *M. tuberculosis* with disease outcome measured by either lesion volume to lung volume ratio (A), lung gross pathology score (B), Chest radiograph score (C), erythrocyte sedimentation rate (D), or survival time post challenge (E). Data points represent individual animals, and vaccination groups are indicated by colour. Spearman's correlation coefficient (*r*) and significance values (*p*) are indicated.

doi:10.1371/journal.pone.0171906.g003

seen across all animals although there was a trend for tissues collected from M998E to have higher bacterial loads than comparable tissues from the other eight macaques (Fig 5).

#### 4. Discussion

This is the first report of the effect of exposure dose on the outcome of infection with *M. tuberculosis* in a more genetically homogeneous species of non-human primate. Mauritian cynomolgus macaques were susceptible to aerosol exposure to *M. tuberculosis*, and displayed clinical signs and disease features similar to those reported in rhesus and Chinese cynomolgus macaques following exposure to the same *M. tuberculosis* strain [30, 31]. All of the challenged Mauritian cynomolgus macaques exhibited clinical signs typical of active human tuberculosis and developed lung lesions with both a gross and microscopic pathology similar to that described previously in TB-infected rhesus and Asian macaques [4, 5, 31, 34]. The key features of the pathological changes were consistent with those described in human infections including a heterogeneity in lesion type and distribution, within and between individuals [35]. The pattern of pulmonary disease was typical of experimental aerosol exposure with lesions distributed throughout the lung [31, 36] while the burden of disease was directly related to the aerosol exposure dose.

In order to make a direct comparison of the disease induced in Mauritian cynomolgus macaques with that in Chinese cynomolgus and rhesus macaques, an analysis of previously published studies was made where the only variable was the macaque type. Whilst the numbers in this study are small, the findings suggest that Mauritian cynomolgus macaques have only a limited ability to control disease, which appears to be lower than that of Chinese cynomolgus macaques and equivalent to, or potentially even less than that of rhesus macaques (Table 5).

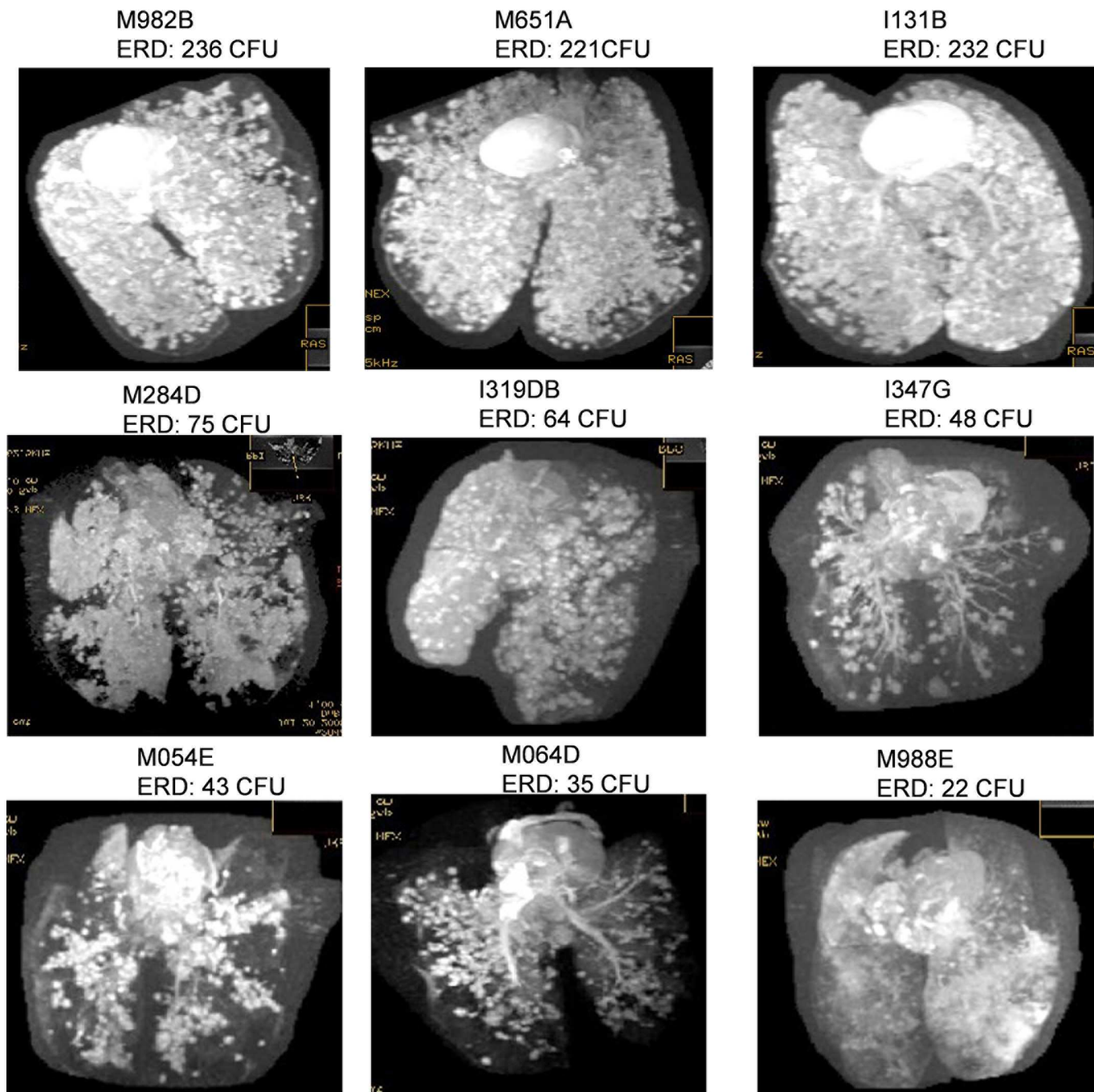


**Fig 4. Magnetic resonance (MR) images of lungs from Mauritian cynomolgus macaques following aerosol infection with a range of doses of *M. tuberculosis*.**

doi:10.1371/journal.pone.0171906.g004

The very high presented aerosol exposure doses (1544–1650 CFU) applied to macaques M982B, I131B, and M651 were selected to match the doses presented (1470–1575 CFU) to rhesus macaques and Chinese cynomolgus macaques in a previously reported study [31] to allow direct comparison of susceptibility among macaque types. Dose comparison between these studies was performed on the basis of the ‘presented dose’ of *M. tuberculosis* rather than the

**Table 3. Summary of lung lesions at dissection of fixed lungs.**

Animal #	Dose (cfu)	Discrete lesions		Coalesced lesions		Range of size of coalesced lesions (mm)	Comments
		right	left	right	left		
M982B	236	TNTC	250	TNTC	18	80% consolidation of right upper 1; 25 x 20 x 15 lesion in right middle. A whole section of left lobe occupied by coalesced lesions.	Multifocal granulomatous pneumonia with extensive coalesced lesions. Fibrous adhesions between lobes. Hilar lymph nodes enlarged and caseous.
I131B	232	TNTC	TNTC	TNTC	TNTC	80–90% consolidation of left lung	Multifocal granulomatous pneumonia with extensive coalesced lesions. Fibrous adhesions between lobes. Left lobes fused
M651A	221	TNTC	TNTC	TNTC	TNTC	80–90% consolidation of left lung	Multifocal granulomatous pneumonia with extensive coalesced lesions. Fibrous adhesions between lobes and with parietal pleura. Left lobes fused
M284D	75	TNTC	TNTC	TNTC	TNTC	8 X 6 to 22 x 12	Lesions too numerous to count and too extensive to measure in right and left lobes. Consolidation estimated as 70–80%. Severe pathology.
I319DB	64	224	TNTC	37	TNTC	4 x 6 to 15 x 18	Lesions too numerous to count and too extensive to measure in left lobes. Consolidation estimated as 80–90%. Widespread fibrous adhesions between upper and lower lobes of right and left lungs. Moderate/severe pathology
I347G	48	TNTC	116	TNTC	9	5 x 4 to 30 x 30	Lesions too numerous to count and too extensive to measure in left lobes. Consolidation estimated as 86–80%. Fibrous adhesions between right lung lobes. Moderate/severe pathology.
M054E	43	150	110	17	15	5 x 5 to 12 x 15	Multifocal granulomatous pneumonia with coalesced lesions. Mild/moderate pathology.
M064D	35	174	110	11	13	5 x 5 to 12 x 10	Multifocal granulomatous pneumonia with coalesced lesions. Mild pathology
M988E	22	74	36	3	10	5 x 8 to 20 x 15	All lobes contained multiple miliary lesions that were too small and numerous to count. Fibrous adhesions were present between left upper and lower lobes. Atypical pathology

TNTC: Too numerous to count.

doi:10.1371/journal.pone.0171906.t003

‘estimated retained dose’, due to refinements only more recently applied to the method to estimate the retained dose [8]. Unlike the three Chinese cynomolgus macaques who controlled disease during the thirteen weeks after very high dose challenge, but similar to the Indian rhesus macaques, progressive disease developed rapidly and endpoint criteria were met seven weeks after challenge in all three of the Mauritian cynomolgus macaques. Both rhesus and Chinese cynomolgus macaques controlled the disease induced following exposure to a high dose challenge of 630 CFU, the lowest dose presented in the study reported by Sharpe et al [31], for the full 13 week post-exposure period. In contrast, Mauritian cynomolgus macaque M284D, the only animal in this study to receive an equivalent high challenge dose, developed disease that met end point criteria ten weeks after challenge and showed a higher level of pulmonary disease measured by lesion: lung volume ratio than that measured in either rhesus or Chinese cynomolgus macaques exposed to similar doses. It is noteworthy that the clinical signs of cough and altered respiratory rates occurred in all Mauritian cynomolgus macaques exposed to high, medium and low doses of TB, but only occurred in a proportion of Indian rhesus macaques and were not seen in Chinese cynomolgus macaques after high dose challenge. Furthermore, one of the Mauritian cynomolgus macaques, (M988E) that received a low challenge dose developed miliary TB which perhaps suggests a lack of ability to adequately control primary infection. Thus, the Mauritian cynomolgus macaques displayed a response to infection

**Table 4. Summary of granuloma distribution.**

Animal	Dose (cfu)	Tissue	Type of granuloma				
			Unorg	Solid	Neutro	Caseated	Coalesced
M982B	236	Hilar LN			+	+	
		Lung	+	+	+	+	
		Liver					
		Kidney			+		
		spleen			+	+	
I131B	232	Hilar LN				+	
		Lung				+	+
		Liver	+	+			
		Kidney		+		+	
		spleen	+	+	+		
M651A	221	Hilar LN				+	
		Lung	+	+	+	+	+
		Liver	+	+	+	+	
		Kidney	+	+	+	+	
		spleen	+	+	+	+	
M284D	75	Hilar LN				+	
		Lung	+	+	+	+	+
		Liver	+				
		Hepatic LN				+	
		Kidneys					
		Spleen					
I319DB	64	Hilar LN				+	
		Lung	+	+	+	+	+
		Liver	+	+	+		
		Kidneys				+	
		Spleen					
1347G	48	Hilar LN				+	
		Lung	+	+	+	+	
		Liver				+	
		Kidneys				+	
		Spleen				+	
M054E	43	Hilar LN				+	
		Lung	+	+	+	+	+
		Liver	+	+			
		Hepatic LN				+	
		Spleen	+	+	+	+	
M064D	35	Hilar LN				+	
		Lung	+	+	+	+	
		Liver	+				
		Hepatic LN	+			+	
		Spleen	+			+	

(Continued)

Table 4. (Continued)

Animal	Dose (cfu)	Tissue	Type of granuloma				
			Unorg	Solid	Neuro	Caseated	Coalesced
M988E	22	Hilar LN				+	
		Lung	+	+	+	+	+
		Liver	+	+			
		Kidneys	+		+	+	
		Spleen				+	

Unorg: Unorganised; Neuro: neutrophic.

doi:10.1371/journal.pone.0171906.t004

which was more like that of rhesus macaques which has been described as a response resembling active TB in susceptible humans [4]. While further work is needed to fully elucidate the difference between these macaque populations, it is clear that geographic origin, as well as species, are important considerations in study design.

The Mauritian cynomolgus macaque has been of particular value in HIV vaccine research [37] where MHC homogeneity has reduced the variability between animals after vaccination and has enhanced comparisons of vaccine regimens. In addition, the improved consistency in outcome has facilitated the use of fewer animals to obtain statistically significant results than if cynomolgus macaques of Chinese or Vietnamese origin were used [37]. In this study, the Mauritian cynomolgus macaques showed less variation in pulmonary disease burden measured as the ratio of lesion volume to lung volume ratio and total gross pathology scores within exposure dose groups, than in either Indian rhesus macaques or Chinese cynomolgus macaques (Table 5). These preliminary observations support the hypothesis that Mauritian cynomolgus macaques could provide a model with a more homogeneous outcome of TB infection. More work is needed to define the variation in outcome of exposure to low or ultra-low aerosol doses and establish an optimal dose for challenge in vaccine efficacy studies.

The Mauritian cynomolgus macaque offers the potential to be an important additional model that could greatly assist the search for correlates of protection and biomarkers of disease that would have an enormous impact on the evaluation of new TB vaccines. Similar to rhesus macaques and Asian cynomolgus macaques, Mauritian cynomolgus macaques made mycobacteria-specific IFN $\gamma$  responses following exposure to *M. tuberculosis* with the frequency of IFN $\gamma$ -producing cells reflecting disease burden and therefore antigen load [8]. However it is the differences in the immune responses made by different macaque populations that provide an important opportunity that could assist with the elucidation of new biomarkers of disease and/or correlates of protection. Further work with state-of-the-art immunological tools will be required to fully characterise the response of the Mauritian cynomolgus macaque to *M. tuberculosis* infection and allow cross genotype and species comparisons to expose the mechanisms responsible for the differences in TB control between macaque species and populations

The genetic homogeneity of the Mauritian cynomolgus macaque population is an asset that offers the opportunity to further understand the immune response to vaccination and infection. The relative ease of MHC haplotype characterisation and the high frequency of selected MHC haplotypes have allowed population studies to be conducted in the HIV field. Possession of specific MHC class I and II haplotypes have been shown to influence the outcome of experimental infection of Mauritian cynomolgus macaques with SHIVSF162P4cy [38], together with the immune response induced [39], and these can be associated with superior viraemic control of SIV or SHIV viruses in naïve-challenged and vaccinated individuals [25–27]. Although the small size of this study prevented meaningful evaluation of the possession of specific MHC

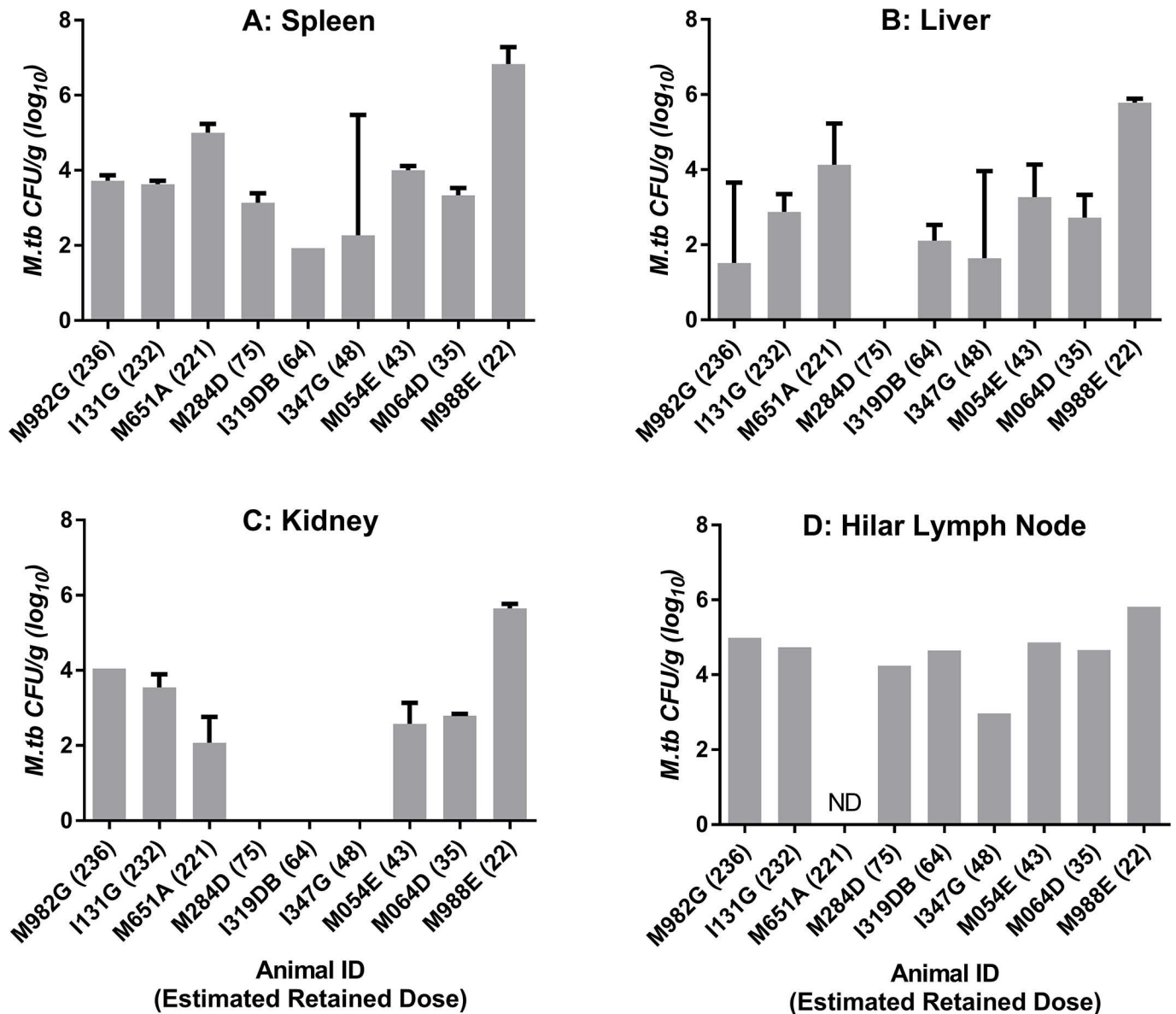


**Fig 5. Bacterial burden in extra-pulmonary tissues collected from Mauritian cynomolgus macaques following aerosol infection with a range of doses of *M. tuberculosis*.** Bars show CFU recovered from samples of spleen (A), liver (B), kidney (C) and Hilar lymph node (D). CFU recovered from replicate tissue samples are shown as a mean with standard deviation indicated as error bars. Samples for which bacteriology analysis was not done (ND) are indicated.

doi:10.1371/journal.pone.0171906.g005

haplotypes on outcome of *M. tuberculosis* infection, statistical power will increase as more studies using this genetic sub-type of the species, presenting the opportunity to identify potential associations.

In conclusion, this study has shown that Mauritian cynomolgus macaque are susceptible to aerosol challenge with *M. tuberculosis*, and develop patterns of disease similar to that reported in cynomolgus macaques of Asian origin but display an increased susceptibility and reduced ability to control disease progression. The predisposition to develop high burden disease, together with, the homogeneity of the occurrence of cough, make this type of macaque an attractive host for studies of TB transmission. The restricted genetic variability of the

**Table 5. Clinical features following aerosol exposure to *M. tuberculosis* in three macaque populations.**

Species	Number in group	Presented Dose range (CFU)	Frequency of contra-indicators % of group showing feature						Lung disease	Total disease burden
			Abnormal Behaviour	Abnormal respiration	In-appetence	Cough	Other indicators	Survival < 12 weeks	Mean Lesion volume: lung volume (range)	Mean Total gross pathology score (range)
MCM	3	Very high [>1400]	67%	100	100	67	100	100	0.33 (0.27–0.37)	35 (33–39)
CCM	3		0	33	0	67	0	0	0.15 (0.04–0.31)	29.3 (22–39)
IRM	3		100	100	67	100	100	100	0.23 (0.13–0.38)	29.7 (21–28)
MCM	1	High	0	100	0	100	0	100	0.28	23
CCM	9		0	0	0	0	0	0	0.04 (0.01–0.14)	16.3 (2–29)
IRM	6	[500–1400]	17	17	17	34	50	17	0.04 (0.02–0.8)	19.5 (14–23)
MCM	3	Medium [250–500]	0	100	0	100	0	0	0.13 (0.12–0.14)	26.7 (22–29)
MCM	2	Low [<250]	50	100	0	100	50	50	0.08 (0.06–0.11)	25 (23–27)

MCM: Mauritian cynomolgus macaque; CCM: Chinese cynomolgus macaque; IRM: Indian rhesus macaque. Other indicators: coat condition, activity level. Data on IRM and CCM from Sharpe *et al* [31]

doi:10.1371/journal.pone.0171906.t005

Mauritian cynomolgus macaque population provides an advantage in the battle to elucidate correlates of protective immunity. Further work is required to develop the Mauritian cynomolgus macaque as a model for the evaluation of TB vaccines, particularly the definition of low and ultra-low aerosol doses suitable for the assessment of vaccine efficacy. However, once established, the benefits of the Mauritian cynomolgus macaque population recognised by the HIV field could be unlocked for TB research.

### Acknowledgments

This work was supported by the Department of Health, UK. The views expressed in this publication are those of the authors and not necessarily those of the Department of Health. We thank the staff of the Biological Investigations Group at PHE Porton for assistance in conducting studies, Alice Marriott, Charlotte Sarfas and Jenny Gullick for assistance with the immune response analysis and Kim Hatch for histology support.

### Author Contributions

**Conceptualization:** SS PM AW MD.

**Data curation:** SS ADW LS FG GH RB AM SC KG PM AW MD.

**Formal analysis:** ADW RB FG.

**Funding acquisition:** SS AW PM MD.

**Investigation:** SS ADW LS FG GH RB AM SC KG PM AW MD.



**Methodology:** SS ADW LS FG GH RB AM SC KG PM AW MD.

**Project administration:** SS MD.

**Resources:** SS ADW LS FG GH RB AM SC KG PM AW MD.

**Supervision:** SS PM AW MD.

**Visualization:** SS ADW LS.

**Writing – original draft:** SS.

**Writing – review & editing:** SS ADW LS FG GH RB AM SC KG PM AW MD.

## References

1. Zumla A, George A, Sharma V, Herbert RHN, Baroness Masham of Ilton, Oxley A, Oliver M. 2015. The WHO 2014 global tuberculosis report—further to go. *Lancet Glob Health* 3:e10–12. doi: [10.1016/S2214-109X\(14\)70361-4](https://doi.org/10.1016/S2214-109X(14)70361-4) PMID: [25539957](https://pubmed.ncbi.nlm.nih.gov/25539957/)
2. Trunz BB, Fine P, Dye C. 2006. Effect of BCG vaccination on childhood tuberculous meningitis and primary tuberculosis worldwide: a meta-analysis and assessment of cost-effectiveness. *Lancet* 367:1173–1180. doi: [10.1016/S0140-6736\(06\)68507-3](https://doi.org/10.1016/S0140-6736(06)68507-3) PMID: [16616560](https://pubmed.ncbi.nlm.nih.gov/16616560/)
3. Colditz GA, Brewer TF, Berkey CS, Wilson ME, Burdick E, Fineberg HV et al. 1994. Efficacy of BCG vaccine in the prevention of tuberculosis. Meta-analysis of the published literature. *JAMA* 271:698–702. PMID: [8309034](https://pubmed.ncbi.nlm.nih.gov/8309034/)
4. Scanga CA, Flynn JL. 2014. Modelling tuberculosis in nonhuman primates. *Cold Spring Harbor Perspect Med* 4:a018564
5. Peña JC, Ho WZ Monkey models of tuberculosis: lessons learned. *Infect Immun*. 2015 Mar; 83(3):852–62. doi: [10.1128/IAI.02850-14](https://doi.org/10.1128/IAI.02850-14) PMID: [25547788](https://pubmed.ncbi.nlm.nih.gov/25547788/)
6. Kaushal D, Mehra S, Didier PJ, Lackner AA. 2012. The non-human primate model of tuberculosis. *J Med Primatol* 41:191–201. Ultra low dose aerosol challenge with *Mycobacterium tuberculosis* leads to divergent outcomes in rhesus and cynomolgus macaques. doi: [10.1111/j.1600-0684.2012.00536.x](https://doi.org/10.1111/j.1600-0684.2012.00536.x) PMID: [22429048](https://pubmed.ncbi.nlm.nih.gov/22429048/)
7. Langermans JA, Andersen P, van Soolingen D, Vervenne RA, Frost PA, van der Laan T et al. Divergent effect of bacillus Calmette-Guérin (BCG) vaccination on *Mycobacterium tuberculosis* infection in highly related macaque species: implications for primate models in tuberculosis vaccine research. *Proc Natl Acad Sci U S A*. 2001 Sep 25; 98(20):11497–502. doi: [10.1073/pnas.201404898](https://doi.org/10.1073/pnas.201404898) PMID: [11562492](https://pubmed.ncbi.nlm.nih.gov/11562492/)
8. Sharpe S, White A, Gleeson F, McIntyre A, Smyth D, Clark S et al. Ultra low dose aerosol challenge with *Mycobacterium tuberculosis* leads to divergent outcomes in rhesus and cynomolgus macaques. *Tuberculosis (Edinb)*. 2016 Jan; 96:1–12.
9. Walsh GP, Tan EV, dela Cruz EC, Abalos RM, Villahermosa LG, Young LJ et al. The Philippine cynomolgus monkey (*Macaca fascicularis*) provides a new non-human primate model of tuberculosis that resembles human disease. *Nat Med* 1996; 2:237–240.
10. Reed SG, Coler RN, Dalemans W, Tan EV, Dela Cruz EC, Basaraba RJ et al. Defined tuberculosis vaccine, Mtb72F/AS02A, evidence of protection in cynomolgus monkeys. *PNAS* 2009; 106: 2301–2306. doi: [10.1073/pnas.0712077106](https://doi.org/10.1073/pnas.0712077106) PMID: [19188599](https://pubmed.ncbi.nlm.nih.gov/19188599/)
11. Sugawara I, Li Z, Sun L, Udagawa T and Taniyama T. Recombinant BCG Tokyo (Ag85A) protects cynomolgus monkeys (*macaca fascicularis*) infected with H37Rv *Mycobacterium tuberculosis*. *Tuberculosis* 2007; 87:518–525. doi: [10.1016/j.tube.2007.06.002](https://doi.org/10.1016/j.tube.2007.06.002) PMID: [17720625](https://pubmed.ncbi.nlm.nih.gov/17720625/)
12. Capuano SV, Croix DA, Pawar S, Zinovic A, Myers A, Lin PL et al. Experimental *Mycobacterium tuberculosis* infection of cynomolgus macaques closely resembles the various manifestations of human *M. tuberculosis* infection. *Infect Immun* 2003; 5831–5844. doi: [10.1128/IAI.71.10.5831-5844.2003](https://doi.org/10.1128/IAI.71.10.5831-5844.2003) PMID: [14500505](https://pubmed.ncbi.nlm.nih.gov/14500505/)
13. Lawler SH, Sussman RW, Taylor LL. Mitochondrial DNA of the Mauritian macaques (*Macaca fascicularis*): an example of the founder effect. *Amer J Phys Anthropol*. 1995; 96:133–141. doi: [10.1002/ajpa.1330960203](https://doi.org/10.1002/ajpa.1330960203) PMID: [7755104](https://pubmed.ncbi.nlm.nih.gov/7755104/)
14. Kanthaswamy S, Ng J, Satkoski Trask J, George DA, Kou AJ, Hoffman LN et al. The genetic composition of populations of cynomolgus macaques (*Macaca fascicularis*) used in biomedical research. *J Med Primatol*. 2013 Jun; 42(3):120–31. doi: [10.1111/jmp.12043](https://doi.org/10.1111/jmp.12043) PMID: [23480663](https://pubmed.ncbi.nlm.nih.gov/23480663/)

15. Drevon-Gaillot E, Perron-Lepage MF, Clement C, Burnett R. A review of background findings in cynomolgus monkeys (*Macaca fascicularis*) from three different geographical origins. *Exp Toxicol Pathol.* 2006; 58:77–88. doi: [10.1016/j.etp.2006.07.003](https://doi.org/10.1016/j.etp.2006.07.003) PMID: [16984807](https://pubmed.ncbi.nlm.nih.gov/16984807/)
16. Luetjens CM, Weinbauer GF. Functional assessment of sexual maturity in male macaques (*Macaca fascicularis*). *Regul Toxicol Pharmacol.* 2012; 63:391–400. doi: [10.1016/j.yrtph.2012.05.003](https://doi.org/10.1016/j.yrtph.2012.05.003) PMID: [22579626](https://pubmed.ncbi.nlm.nih.gov/22579626/)
17. Bourges-Abella N, Geffre A, Moureaux E, Vincenti M, Braun JP, Trumel C. Hematologic reference intervals in cynomolgus (*Macaca fascicularis*) monkeys. *J Med Primatol.* 2014; 43:1–10. doi: [10.1111/jmp.12077](https://doi.org/10.1111/jmp.12077) PMID: [24102586](https://pubmed.ncbi.nlm.nih.gov/24102586/)
18. Seekatz AM, Panda A, Rasko DA, Toapanta FR, Eloë-Fadrosch EA, Khan AQ et al. Differential response of the cynomolgus macaque gut microbiota to *Shigella* infection. *PLoS One.* 2013 Jun 5; 8(6).
19. Krebs KC, Jin Z, Rudersdorf R, Hughes AL, O'Connor DH. Unusually high frequency MHC class I alleles in Mauritian origin cynomolgus macaques. *J Immunol.* 2005; 175:5230–523. PMID: [16210628](https://pubmed.ncbi.nlm.nih.gov/16210628/)
20. O'Connor SL, Blasky AJ, Pendley CJ, Becker EA, Wiseman RW, Karl JA et al. Comprehensive characterization of MHC class II haplotypes in Mauritian cynomolgus macaques. *Immunogenetics.* 2007; 59:449–462. doi: [10.1007/s00251-007-0209-7](https://doi.org/10.1007/s00251-007-0209-7) PMID: [17384942](https://pubmed.ncbi.nlm.nih.gov/17384942/)
21. Wiseman RW, Wojcechowskyj JA, Greene JM, Blasky AJ, Gopon T, Soma T et al. Simian immunodeficiency virus SIVmac239 infection of major histocompatibility complex-identical cynomolgus macaques from Mauritius. *J Virol.* 2007; 81:349–61. doi: [10.1128/JVI.01841-06](https://doi.org/10.1128/JVI.01841-06) PMID: [17035320](https://pubmed.ncbi.nlm.nih.gov/17035320/)
22. O'Connor S, Lhost JL, Becker EA, Detmer AM, Johnson RC, Macnair CE et al. MHC heterozygote advantage in simian immunodeficiency virus-infected Mauritian cynomolgus macaques. *Sci Trans Med.* 2010; 2:22ra18.
23. Greene JM, Lhost JL, Burwitz BJ, Budde ML, Macnair CE, Weiker MK, Rakasz EG et al. Extralymphoid CD8+ T cells resident in tissues from simian immunodeficiency virus SIVmac239Δnef-vaccinated macaques suppress SIVmac239 replication ex vivo. *J Virol.* 2010; 84(7):3362–3372. doi: [10.1128/JVI.02028-09](https://doi.org/10.1128/JVI.02028-09) PMID: [20089651](https://pubmed.ncbi.nlm.nih.gov/20089651/)
24. Greene JM, Burwitz BJ, Blasky AJ, Mattila TL, Hong JJ, et al. Allogeneic lymphocytes persist and traffic in feral MHC-matched Mauritian cynomolgus macaques. *PLoS ONE.* 2008; 3:e2384 doi: [10.1371/journal.pone.0002384](https://doi.org/10.1371/journal.pone.0002384) PMID: [18545705](https://pubmed.ncbi.nlm.nih.gov/18545705/)
25. Florese RH, Wiseman RW, Venzon D, Karl JA, Demberg T, Larsen K et al. Comparative study of Tat vaccine regimens in Mauritian cynomolgus and Indian rhesus macaques: influence of Mauritian MHC haplotypes on susceptibility/resistance to SHIV(89.6P) infection. *Vaccine.* 2008; 26:3312–3321. doi: [10.1016/j.vaccine.2008.03.100](https://doi.org/10.1016/j.vaccine.2008.03.100) PMID: [18486283](https://pubmed.ncbi.nlm.nih.gov/18486283/)
26. Mee ET, Berry N, Ham C, Sauermann U, Maggiorella MT, Martinan F et al. Mhc haplotype H6 is associated with sustained control of SIVmac251 infection in Mauritian cynomolgus macaques. *Immunogenetics.* 2009; 61:327–339. doi: [10.1007/s00251-009-0369-8](https://doi.org/10.1007/s00251-009-0369-8) PMID: [19337730](https://pubmed.ncbi.nlm.nih.gov/19337730/)
27. Mee ET, Berry N, Ham C, Aubertin A, Lines J, Hall J et al. Mhc haplotype M3 is associated with early control of SHIVsbg infection in Mauritian cynomolgus macaques. *Tissue Antigens.* 2010; 76:223–229. doi: [10.1111/j.1399-0039.2010.01500.x](https://doi.org/10.1111/j.1399-0039.2010.01500.x) PMID: [20403147](https://pubmed.ncbi.nlm.nih.gov/20403147/)
28. Mee ET, Badhan A, Karl JA, Wiseman RW, Cutler K, Knapp LA, et al. MHC haplotype frequencies in a UK breeding colony of Mauritian cynomolgus macaques mirror those found in a distinct population from the same geographic origin. *J Med Primatol.* 2009 Feb; 38(1):1–14. doi: [10.1111/j.1600-0684.2008.00299.x](https://doi.org/10.1111/j.1600-0684.2008.00299.x) PMID: [19018947](https://pubmed.ncbi.nlm.nih.gov/19018947/)
29. Clark SO, Hall Y, Kelly DIF, Hatch GJ, Williams A. Survival of *Mycobacterium tuberculosis* during experimental aerosolization and implications for aerosol challenge models. *J. Appl. Microbiol.* 111 (2011) 350–359. doi: [10.1111/j.1365-2672.2011.05069.x](https://doi.org/10.1111/j.1365-2672.2011.05069.x) PMID: [21651681](https://pubmed.ncbi.nlm.nih.gov/21651681/)
30. Sharpe SA, McShane H, Dennis MJ, Basaraba RJ, Gleeson F, Hall G et al. Establishment of an aerosol challenge model of tuberculosis in rhesus macaques and an evaluation of endpoints for vaccine testing. *Clin. Vaccine Immunol. CVI.* 17 (2010) 1170–82. doi: [10.1128/CVI.00079-10](https://doi.org/10.1128/CVI.00079-10) PMID: [20534795](https://pubmed.ncbi.nlm.nih.gov/20534795/)
31. Sharpe SA, Eschelbach E, Basaraba RJ, Gleeson F, Hall GA, McIntyre A et al. Determination of lesion volume by MRI and stereology in a macaque model of tuberculosis. *Tuberculosis.* 89 (2009) 405–416. doi: [10.1016/j.tube.2009.09.002](https://doi.org/10.1016/j.tube.2009.09.002) PMID: [19879805](https://pubmed.ncbi.nlm.nih.gov/19879805/)
32. Druett HA. A mobile form of the Henderson apparatus. *J. Hyg. (Lond.).* 67 (1969) 437–48.
33. Harper GJ, Morton JD. The respiratory retention of bacterial aerosols: experiments with radioactive spores. *Epidemiol. Infect.* 51 (1953) 372–385.
34. Lin PL, Pawar S, Myers A, Pergu A, Fuhrman C, Reinhart TA et al. Early events in *Mycobacterium tuberculosis* infection in cynomolgus macaques *Infect Immun* 2006; 74, 3790–3803.
35. Basaraba RJ. Experimental tuberculosis: the role of comparative pathology in the discovery of improved tuberculosis treatment strategies. *Tuberculosis,* 88 (Suppl. 1) (2008), pp. S35–S47

36. Sibley L, Dennis M, Sarfas C, White A, Clark S, Gleeson F et al. Route of delivery to the airway influences the distribution of pulmonary disease but not the outcome of *Mycobacterium tuberculosis* infection in rhesus macaques. *Tuberculosis (Edinb)*. 2016 Jan; 96:141–9.
37. Sui Y, Gordon S, Franchini G, Berzofsky JA. Nonhuman primate models for HIV/AIDS vaccine development. *Curr Protoc Immunol*. 2013 Oct 1; 102:Unit 12.14.
38. Borsetti A, Ferrantelli F, Maggiorella MT, Sernicola L, Bellino S, Gallinaro A, Farcomeni S, Mee ET, Rose NJ, Cafaro A, Titti F, Ensoli B. Effect of MHC haplotype on immune response upon experimental SHIVSF162P4cy infection of Mauritian cynomolgus macaques. *PLoS One*. 2014 Apr 2; 9(4):e93235. doi: [10.1371/journal.pone.0093235](https://doi.org/10.1371/journal.pone.0093235) PMID: [24695530](https://pubmed.ncbi.nlm.nih.gov/24695530/)
39. Borsetti A, Maggiorella MT, Sernicola L, Bellino S, Ferrantelli F, Belli R et al. Influence of MHC class I and II haplotypes on the experimental infection of Mauritian cynomolgus macaques with SHIVSF162P4cy. *Tissue Antigens*. 2012 Jul; 80(1):36–45. doi: [10.1111/j.1399-0039.2012.01875.x](https://doi.org/10.1111/j.1399-0039.2012.01875.x) PMID: [22494179](https://pubmed.ncbi.nlm.nih.gov/22494179/)